tra (this is difficult to discern from Fig. 2). This could be due to the use of the pinhole microphone (as suggested by Ref. 8). However, the effect of the tandem LEBUs is seen in the lower part of the region where the pinhole and piezoelectric transducer measurements differ. These data show a net reduction of p_w' of 12.5%. It is noted that LEBU device noise could be another source of error in the high-frequency $\phi(\omega)$ measured (due to dynamic flow separation on the LEBUs). Notice that vibration does not affect the measurement significantly in the region of the measured effects.

Conclusions

An initial measurement of p_w' downstream of tandem LEBUs show a significant reduction compared to the reference flat plate case. The average magnitude of the p_w' reduction is 12.5%. The peak reduction is at 7-8 kHz and is on the order of the C_f reduction due to the tandem LEBUs (25%). Since the measurement is at only one location, device noise and other effects (such as downstream extent/relaxation) could not be evaluated. These data provide an indication of a secondary benefit of LEBUs (in addition to their skin-friction reduction performance).

References

[1]Urick, R., *Principles of Underwater Sound*, 3rd ed., McGraw-Hill Book Co., New York, 1983, p. 365.

[2]Greshilov, E.M., Evtushenko, A.V., and Lyamshev, L.M., "Hydrodynamic Noise and Toms Effect," *Soviet Physics - Acoustics*, Vol. 21, No. 3, 1975, pp. 396-404.

[3]Bhat, W.V. and Wilby, J.B., "Interior Noise Radiated by an Airplane Fuselage Subjected to Turbulent Boundary Layer Excitation and Evaluation of Noise Reduction Treatments," *Journal of Sound and Vibration*, Vol. 18, No. 4, 1971, pp. 449-454.

[4]Anders, J.B., Hefner, J.N., and Bushnell, D.M., "Performance of Large-Eddy Breakup Devices at Post Transition Reynolds Numbers," AIAA Paper 84-0345, Jan. 1984.

[5]Thomas, A.S.W., "Organized Structures in the Turbulent Boundary Layer," Ph.D. Dissertation, University of South Adelaide, Australia, 1977.

[6]Hefner, J.N., Weinstein, L.M., and Bushnell, D.M., "Large-Eddy Breakup Scheme for Turbulent Viscous Drag Reduction," *Progress in Astronautics and Aeronautics: Viscous Flow Drag Reduction*, Vol. 72, edited by Gary R. Hough, AIAA, New York, 1981, pp. 118-127.

[7]Hefner, J.N., Anders, J.B., and Bushnell, D.M., "Alteration of Outer Flow Structures for Turbulent Drag Reduction," AIAA Paper 83-0293, Jan. 1983.

[8]Bull, M.K. and Thomas, A.S.W., "High Frequency Wall Pressure Fluctuations in Turbulent Boundary Layers," *Physics of Fluids*, Vol. 19, April 1976, pp. 597-599.

Quasilinear Form of Rankine-Hugoniot Jump Conditions

Czeslaw P. Kentzer*
Purdue University, West Lafayette, Indiana

THIS Note shows that the generalized Rankine-Hugoniot jump conditions associated with the divergence (or "conservative") form of the Euler equations of gasdynamics may be put in the equivalent form corresponding to the quasilinear (or "nonconservative") form. Associating a proper set of algebraic jump conditions directly with a given set of differential equations is crucial in numerical computations according to Lax,[1] and may be conveniently formalized using Emde's notation,[2] namely, associating a volume (differential) operator with an appropriate surface (algebraic) multiplication operator. In computational gasdynamics the usefulness of such an association goes beyond mere notation. This is so because finite approximations may be viewed as algebraic operators replacing (approximating) differential operators and may be chosen so as to collapse automatically to the correct jump conditions in the presence of discontinuities. This property of finite difference schemes was demonstrated earlier[3] for the case of the divergence form of the Euler system. Here we demonstrate the technique of obtaining the quasilinear jump conditions corresponding to a given quasilinear form of the Euler system. The intention is to publicize the possibilities of constructing difference schemes approximating simultaneously the differential equations and the jump conditions for all forms of the Euler system of gasdynamics.

We shall start with the divergence form of the Euler equations,

$$\frac{\partial \rho}{\partial t} + \nabla \cdot (\rho \boldsymbol{u}) = 0, \qquad \frac{\partial \rho \boldsymbol{u}}{\partial t} + \nabla \cdot (\rho \boldsymbol{u}\boldsymbol{u}) + \nabla p = 0$$

$$\frac{\partial \rho e^\circ}{\partial t} + \nabla \cdot (\rho h^\circ \boldsymbol{u}) = 0 \tag{1}$$

where ρ is the mass density, $\boldsymbol{u}$ the velocity, p the pressure, e° the total specific internal energy, and $h^\circ = e^\circ + p/\rho$ the total specific enthalpy.

Equation (1) allows for the use of Emde's notation, namely, in the presence of a surface of discontinuity Σ, the differential system (1) must be replaced by an algebraic system formally obtained from the first by replacing volume differential operators $\partial/\partial t$ and ∇ by the surface algebraic multiplication operators $-U$ and $\boldsymbol{n}$, respectively, which operate on the differences (jumps) in the differentiated functions across the singular surface. The jumps are surface functions, i.e., functions of position on Σ. Thus, using Emde's notation, we obtain from Eq. (1) the known result (see, e.g., Ref. 4), namely,

$$-U[\rho] + \boldsymbol{n}\cdot[\rho \boldsymbol{u}] = 0, \qquad -U[\rho \boldsymbol{u}] + \boldsymbol{n}\cdot[\rho \boldsymbol{u}\boldsymbol{u}] + \boldsymbol{n}[p] = 0$$

$$-U[\rho e^\circ] + \boldsymbol{n}\cdot[\rho h^\circ \boldsymbol{u}] = 0 \tag{2}$$

where $\boldsymbol{n}$ is the unit spatial normal to the discontinuity, U the displacement speed of the discontinuity in the direction of $\boldsymbol{n}$, and $[\psi] = \psi_2 - \psi_1$ is the jump in ψ across the surface Σ.

Quasilinear forms of the Euler system of gasdynamics may be obtained directly from the divergence form [Eq. (1)] by applying rules for the derivatives of products, subtraction of multiples of mass or momentum equations, and rearrangement of terms. We shall perform parallel operations on the algebraic jump conditions (2). For this we need the following:

$$[ab] = a_2 b_2 - a_1 b_1$$

$$= a_2 b_2 - a_2 b_1 + a_2 b_1 - a_1 b_1 = a_2[b] + b_1[a]$$

$$= a_2 b_2 - a_1 b_2 + a_1 b_2 - a_1 b_1 = a_1[b] + b_2[a]$$

Preferring expressions symmetric in subscripts, we average and write

$$[ab] = \langle a \rangle [b] + \langle b \rangle [a]$$

where $\langle a \rangle = (a_2 + a_1)/2 =$ the arithmetic average of a. Note the analogy of the above to the formula $\delta(ab) = a\delta(b) + b\delta(a)$. We will need also the geometric mean, defined as

Received June 17, 1985.

*Associate Professor of Aeronautics and Astronautics. Member AIAA.

$\tilde{a} = (a_2 a_1)^{1/2}$, by means of which we may further write

$$\langle 1/a \rangle = \langle a \rangle / \tilde{a}^2$$

for the arithmetic average of the inverse. Now we may proceed formally expanding the jumps of products of the primitive variables appearing in Eq. (2).

The mass balance across Σ is

$$-U[\rho] + \boldsymbol{n}\cdot[\rho \boldsymbol{u}] = -U[\rho] + \langle \boldsymbol{u}\rangle \cdot \boldsymbol{n}[\rho] + \langle \rho \rangle \boldsymbol{n}\cdot[\boldsymbol{u}]$$
$$= (-U + \langle \boldsymbol{u}\rangle \cdot \boldsymbol{n})[\rho] + \langle \rho \rangle \boldsymbol{n}\cdot[\boldsymbol{u}] = 0 \tag{3a}$$

The above corresponds formally to

$$\frac{D\rho}{Dt} + \rho \nabla \cdot \boldsymbol{u} = \left(\frac{\partial}{\partial t} + \boldsymbol{u}\cdot\nabla\right)\rho + \rho\nabla\cdot\boldsymbol{u} = 0 \tag{3b}$$

Eq. (3a) is linear in the jumps $[\rho]$ and $[\boldsymbol{u}]$ and may be obtained directly from the corresponding differential equation (3b) using Emde's notation and proper averaging of the coefficients. Other useful forms of Eq. (3a) follow from moving the surface functions, such as U, $\boldsymbol{n}$, and the averages, inside the square brackets:

$$-U[\rho] + \boldsymbol{n}\cdot[\rho\boldsymbol{u}] = [\rho(-U + \boldsymbol{n}\cdot\boldsymbol{u})] = [m] = m_2 - m_1 = 0$$

showing that the relative mass flux $m = \rho(-U + \boldsymbol{n}\cdot\boldsymbol{u})$ is conserved across Σ. This implies immediately that

$$m = \langle m \rangle = -U\langle \rho \rangle + \boldsymbol{n}\cdot\langle \rho\boldsymbol{u}\rangle \tag{4}$$
$$= (\rho_1 m_2 + \rho_2 m_1)/(\rho_2 + \rho_1)$$
$$= \rho_2\rho_1(-2U + \boldsymbol{n}\cdot\boldsymbol{u}_2 + \boldsymbol{n}\cdot\boldsymbol{u}_1)/(\rho_2 + \rho_1)$$

so that, in Emde's notation, a multiplication by

$$m = (-U + \boldsymbol{n}\cdot\langle \boldsymbol{u}\rangle)/\langle 1/\rho\rangle \tag{5}$$

corresponds formally to $\rho(D/Dt)$ or to differentiation following the fluid and multiplication of the result by density.

Turning now to the momentum balance across Σ, we have

$$-U[\rho\boldsymbol{u}] + \boldsymbol{n}\cdot[\rho\boldsymbol{u}\boldsymbol{u}] + \boldsymbol{n}[p] = \langle \boldsymbol{u}\rangle\{-U[\rho] + \boldsymbol{n}\cdot[\rho\boldsymbol{u}]\}$$
$$+ (-U\langle\rho\rangle + \langle\rho\boldsymbol{u}\rangle\cdot\boldsymbol{n})[\boldsymbol{u}] + \boldsymbol{n}[p] = 0$$

The first term in brackets vanishes by virtue of Eq. (3a). Using Eqs. (4) and (5), the momentum balance becomes, upon multiplication by $\langle 1/\rho\rangle$,

$$(-U + \langle\boldsymbol{u}\rangle\cdot\boldsymbol{n})[\boldsymbol{u}] + \langle 1/\rho\rangle\boldsymbol{n}[p] = 0 \tag{6a}$$

which is the analog of the quasilinear momentum equation

$$\frac{D\boldsymbol{u}}{Dt} + \frac{1}{\rho}\nabla p = 0 \tag{6b}$$

The energy balance across Σ, when expanded, is

$$-U[\rho e^\circ] + \boldsymbol{n}\cdot[\rho\boldsymbol{u}e^\circ] + \boldsymbol{n}\cdot[p\boldsymbol{u}] = \langle e^\circ\rangle\{-U[\rho] + \boldsymbol{n}\cdot[\rho\boldsymbol{u}]\}$$
$$+ (-U\langle\rho\rangle + \langle\rho\boldsymbol{u}\rangle\cdot\boldsymbol{n})[e^\circ] + \langle\boldsymbol{u}\rangle\cdot\boldsymbol{n}[p]$$
$$+ \langle p\rangle\boldsymbol{n}\cdot[\boldsymbol{u}] = 0$$

But $[e^\circ] = [e] + [\tfrac{1}{2}\boldsymbol{u}\cdot\boldsymbol{u}] = [e] + \langle\boldsymbol{u}\rangle\cdot[\boldsymbol{u}]$, so that, after dropping the first term on the right on account of Eq. (3a), we have

$$(-U\langle\rho\rangle + \langle\rho\boldsymbol{u}\rangle\cdot\boldsymbol{n})[e] + \langle p\rangle\boldsymbol{n}\cdot[\boldsymbol{u}]$$
$$+ \langle\boldsymbol{u}\rangle\cdot\{(-U\langle\rho\rangle + \langle\rho\boldsymbol{u}\rangle\cdot\boldsymbol{n})[\boldsymbol{u}] + \boldsymbol{n}[p]\} = 0$$

Here the last term in brackets vanishes by virtue of momentum balance, Eq. (6a). Multiplying by $\langle 1/\rho\rangle$, we have

$$(-U + \langle\boldsymbol{u}\rangle\cdot\boldsymbol{n})[e] + \langle 1/\rho\rangle\langle p\rangle\boldsymbol{n}\cdot[\boldsymbol{u}] = 0 \tag{7a}$$

which is the surface analog of the differential equation

$$\frac{De}{Dt} + \frac{p}{\rho}\nabla\cdot\boldsymbol{u} = 0 \tag{7b}$$

Substituting for $\boldsymbol{n}\cdot[\boldsymbol{u}]$ from Eq. (3), and observing that

$$\left\langle\frac{1}{\rho}\right\rangle\frac{[\rho]}{\langle\rho\rangle} = \frac{1}{\rho_2\rho_1}[\rho] = -\left[\frac{1}{\rho}\right] \tag{8}$$

we have

$$(-U + \langle\boldsymbol{u}\rangle\cdot\boldsymbol{n})[e] + \langle p\rangle(-U + \langle\boldsymbol{u}\rangle\cdot\boldsymbol{n})[1/\rho] = 0 \tag{9a}$$

in analogy to

$$\frac{De}{Dt} + p\frac{D(1/\rho)}{Dt} = 0 \tag{9b}$$

Specializing to a perfect gas,

$$[e] = \frac{1}{\gamma - 1}\left[\frac{p}{\rho}\right] = \frac{1}{\gamma - 1}\left\{\langle p\rangle\left[\frac{1}{\rho}\right] + \left\langle\frac{1}{\rho}\right\rangle[p]\right\}$$

we have from Eq. (9a) using Eq. (8)

$$(-U + \langle\boldsymbol{u}\rangle\cdot\boldsymbol{n})[p] - \frac{\gamma\langle p\rangle}{\langle\rho\rangle}(-U + \langle\boldsymbol{u}\rangle\cdot\boldsymbol{n})[\rho] = 0 \tag{10a}$$

which is the surface analog of

$$\frac{Dp}{Dt} - a^2\frac{D\rho}{Dt} = 0 \tag{10b}$$

with

$$\frac{\gamma\langle p\rangle}{\langle\rho\rangle} = \frac{\langle\rho a^2\rangle}{\langle\rho\rangle}$$

being the correct mass-weighted average of the square of the speed of sound, or the surface equivalent of a^2.

Equations (3a), (6a), (7a), (9a), and, for a perfect gas, (10a), are the algebraic surface analogs of the quasilinear differential equations of Euler, the companion equations (3b), (6b), (7b), (9b), and (10b). Since both sets of equations, algebraic and differential, are derivable from the conservation law forms (2) and (1) by identical sequence of steps, they are equivalent to (2) and (1) when taken together. This we interpret to mean that the necessary condition for the balance of mass, momentum, and energy is to satisfy the differential equations throughout the volume and the *corresponding* jump conditions everywhere on the surface of any discontinuity that may exist. The particular form of the Euler system does not matter.

Of special interest is the fact that the derived algebraic surface relations are *linear* in the finite differences $[\psi] = \psi_2 - \psi_1$, which differences remain finite across a discontinuity. Thus, they may serve as the basis for construction of finite difference schemes approximating Euler equations linear in derivatives of the primitive variables. With properly averaged coefficients, numerical schemes for the quasilinear Euler system, correctly applied, are capable of satisfying the balance of mass, momentum, and energy across any discontinuity. Similar results may be obtained by the procedure described here for the full Navier-Stokes equations for which the jump conditions are known; see, e.g., Green and Naghdi.[5]

References

[1]Lax, P. D., "Hyperbolic Systems of Conservation Laws and the Mathematical Theory of Shock Waves," *SIAM Regional Conference Series in Applied Mathematics*, Vol. 11, SIAM, 1973.

[2]Emde, F., "Zur Vektorenrechnung," *Archiv der Mathematik und Physik*, III Reihe, XXIV, 1915, pp. 1-11.

[3]Kentzer, C. P., "Shock-Point Operator in Conservative Differencing," *Proceedings of NASA Symposium on Numerical Boundary Condition Procedures*, NASA CP, 1982, pp. 389-401.

[4]Majda, A., "Compressible Fluid Flow and Systems of Conservation Laws in Several Space Variables," *Applied Mathematical Sciences*, Vol. 53, Springer-Verlag, New York, 1984, pp. 2-3.

[5]Green, A. E. and Naghdi, P. M., "On the Derivation of Discontinuity Conditions in Continuum Mechanics," *International Journal of Engineering Science*, Vol. 2, March 1965, pp. 621-624.

Frequency Characteristics of Discrete Tones Generated in a High Subsonic Jet

Y. Umeda,* H. Maeda,† and R. Ishii‡
Kyoto University, Kyoto, Japan

Introduction

THE generation mechanism of jet noise was explained theoretically by Lighthill[1] using an idea of quadrupole oscillation of turbulent vortices in a jet; since then, many investigators have reported on sound waves that are emitted when a solid body is placed in a jet. Sometimes it is observed that strong sound waves with particular frequencies are emitted when a solid body is placed in a jet flow. These sound waves with narrow frequency band are called discrete tones. For the generation of such discrete tones, it is required that some proper mechanism exist for a flowfield to resonate at a particular frequency. Discrete tones such as edge tones,[2] blade tones,[3] and cavity tones[4] belong to the same category. Recently, the discrete tones radiated from the high subsonic jet impinging on a flat plate[5] have been investigated.

In our investigation, a new type of discrete tone is found experimentally. This discrete tone is radiated when a slender circular cylinder or a thin flat plate is placed in a high subsonic jet at right angles to the jet axis near the circular nozzle exit. The frequency characteristics of this discrete tone are different in some respects from those of other types of discrete tones investigated previously. This paper describes the frequency characteristics of this discrete tone found in our experiment.

Experimental Apparatus

A schematic view of the experimental apparatus for the generation of the discrete tone is shown in Fig. 1a. A high subsonic air jet was exhausted from a circular nozzle with an internal diameter $d = 1.0$ cm. The jet-exhausted Mach number was regulated by a control valve. A slender circular cylinder or a thin flat plate was mounted on a traverse mechanism set along the jet axis (ξ axis). The nozzle-to-cylinder (or plate) distance x was remotely controlled by a pulse motor. The cross sections of the cylinder and the plate are shown in Fig. 1b. The system was located in a simplified anechoic chamber, where urethan foam was applied to the interior walls and the floor.

Measurements of sound pressure were made by using a 0.32-cm-diam Bruel and Kjaer type-4135 condenser microphone. The microphone was located at a fixed position in the backward arc about 50 deg from the jet axis, at a radius of 1.35 m from the nozzle exit, and 1.50 m above the floor. The experiments for the frequency characteristics of this discrete tone were carried out for the following conditions:

1) The Mach number M of the jet at the nozzle exit is fixed, and the nozzle-to-cylinder (or plate) distance x is changed.

2) The nozzle-to-cylinder (or plate) distance x is fixed, and the flow Mach number M of the jet is changed.

Results and Discussion

Figure 2a shows a spectrum of the jet noise that has broad frequency band only. When the discrete tones are radiated, the spectrum has some sharp peaks at the resonance frequencies in addition to the broad frequency band as shown in Fig. 2b. The dominant frequencies of sound waves in the spectral curve are called the resonance frequencies and are denoted by f. In Fig. 3a, the resonance frequencies f of the discrete tone were plotted against the nozzle-to-cylinder distance x/d for $M = 0.886$, where d is the nozzle diameter. In Fig. 3b, the resonance frequencies f of the discrete tone were plotted against the flow Mach number M for $x/d = 2.0$. It is observed that the results for the flat plate are very similar to the corresponding results for the cylinder. In these figures, black circles represent the frequencies of sounds with prominent peaks whose sound pressure levels exceed those of broad frequency band by 10 dB or more, and white circles represent the frequencies of sounds with small peaks whose sound pressure level exceed those of broad frequency band by 5-10 dB. From these experimental results shown in Figs. 3a and b, it is found that the discrete tone has the following characteristics:

1) This tone is generated when the nozzle-to-cylinder distance x/d is in the range 0.5-8.0 and a jet is operated at $M \geq 0.6$.

2) When the Mach number M of a jet at the nozzle exit is fixed, the observed resonance frequency of the discrete tones decreases gradually as the nozzle-to-cylinder distance is increased. The resonance frequency decreases until a certain

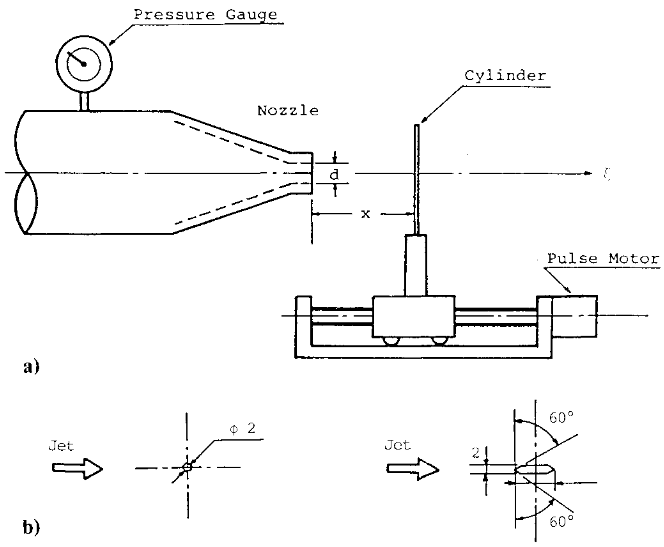

Fig. 1 a) Experimental apparatus for the generation of discrete tone; (ξ: flow direction); b) geometry of a slender circular cylinder and a thin plate (arrow shows flow direction).

Received June 17, 1985.

*Research Associator, Dept. of Aeronautical Engineering.
†Professor, Dept. of Aeronautical Engineering. Member AIAA.
‡Research Associator, Dept. of Aeronautical Engineering. Member AIAA.